Canadian Mineralogist
Vol. 31, pp. 425-436 (1993)

ZINCIAN ILMENITE – ECANDREWSITE FROM A PELITIC SCHIST, DEATH VALLEY, CALIFORNIA, AND THE PARAGENESIS OF (Zn,Fe)TiO_3 SOLID SOLUTION IN METAMORPHIC ROCKS

DONNA L. WHITNEY*

Department of Geology & Geophysics, University of Calgary, Calgary, Alberta T2N 1N4

MARC HIRSCHMANN

Division of Geological and Planetary Science 170–25, California Institute of Technology, Pasadena, California 91125, U.S.A.

MARTIN G. MILLER

Department of Geological Sciences, AJ–20, University of Washington, Seattle, Washington 98195, U.S.A.

ABSTRACT

Two compositionally and petrographically distinct populations of ilmenite–ecandrewsite solid solution, $FeTiO_3$ – $ZnTiO_3$, coexist in a kyanite-bearing schist from the Black Mountains, Death Valley, California. The first population is extremely zinc-rich and has the stoichiometric formula $(Zn_{0.17-0.81}Fe_{0.18-0.64}Mn_{0.01})TiO_3$. Single grains span the entire compositional range. The mineral is orange-brown in transmitted light, and occurs both as inclusions in garnet and as an abundant phase (~3–5 modal %) in the matrix. The second population is opaque in transmitted light, occurs exclusively as a matrix phase, and has the stoichiometric formula $(Zn_{0-0.12}Fe_{0.85-0.98}Mn_{0.01-0.02})TiO_3$. Single grains are generally homogeneous, but there is compositional variation among grains. The paragenesis of zinc-bearing ilmenite solid-solution in metapelitic rocks is problematic. Thermodynamic calculations and comparison with other reported occurrences indicate that ilmenite with greater than a few mol% $ZnTiO_3$ component in metapelitic rocks should be metastable relative to gahnite + quartz + rutile over the range of geologically relevant conditions of regional metamorphism.

Keywords: zinc, ilmenite, ecandrewsite, metapelitic rocks, Death Valley, California.

SOMMAIRE

Deux membres de la solution solide ilménite – ecandrewsite ($FeTiO_3$–$ZnTiO_3$), distincts non seulement en composition mais aussi en aspects texturaux, coexistent dans un schiste à kyanite provenant des Black Mountains, Death Valley, Californie. Le premier groupe est riche en zinc et répond à la formule stoechiométrique $(Zn_{0.17-0.81}Fe_{0.18-0.64}Mn_{0.01})_{\Sigma 1.00}TiO_3$. Un seul grain peut contenir l'intervalle complet de compositions. Le minéral est orange brunâtre en lumière transmise, et se trouve en inclusions dans le grenat et comme phase répandue (~3–5% par volume) dans la matrice. Les grains du second groupe sont opaques en lumière transmise, se trouvent seulement dans la matrice, et répondent à la formule stoechiométrique $(Zn_{0-0.12}Fe_{0.85-0.98}Mn_{0.01-0.02})_{\Sigma 1.00}TiO_3$. Chaque grain est homogène, en général, mais nous décelons une variation parmi les grains. La paragenèse de la solution solide (Zn,Fe)TiO_3 dans les roches métapélitiques est énigmatique. Les calculs thermodynamiques et une comparaison avec les exemples pris de la littérature montrent que l'ilménite ayant plus de quelque pourcents du pôle $ZnTiO_3$ dans les roches pélitiques devrait être métastable par rapport à l'assemblage gahnite + quartz + rutile dans un intervalle réaliste de conditions du métamorphisme régional.

(Traduit par la Rédaction)

Mots-clés: zinc, ilménite, ecandrewsite, roches métapélitiques, Death Valley, Californie.

---

*Present address: Department of Geology and Geography, Vassar College, Poughkeepsie, New York 12601, U.S.A.

INTRODUCTION

We report a new occurrence of ilmenite–ecandrewsite solid solution from a kyanite-bearing schist from Death Valley, California; compositions range from $FeTiO_3$ (ilmenite) to $(Zn_{0.81}Fe_{0.18}Mn_{0.01})TiO_3$ (ecandrewsite). Zincian ilmenite (<50 mol% $ZnTiO_3$) and ecandrewsite (>50 mol% $ZnTiO_3$) have previously been reported from four localities (Table 1), which involve metasedimentary rocks. Because ilmenite typically is not a host of significant amounts of zinc in metamorphic rocks, the paragenesis of zincian ilmenite – ecandrewsite solid solution is of interest.

TABLE 1. LOCALITIES AND COMPOSITIONS OF ZINCIAN ILMENITE AND ECANDREWSITE

LOCALITY	COMPOSITION	ROCK TYPE	REF.
Broken Hill, NSW (Hores Gneiss)	$(Zn_{0.59}Fe_{0.24}Mn_{0.17})TiO_3$	quartz schist	1
(Parnell Fm)	$(Zn_{0.0-0.41}Fe_{0.51-1.0}Mn_{0.0-.05})TiO_3$		2
San Valentin, Spain	$(Zn_{0.55-0.69}Fe_{0.19-0.30}Mn_{0.10-0.13})TiO_3$	oxide-sulfate ore	1
Fuzhou, China	$(Zn_{0.01-0.14}Fe_{0.24-0.53}Mn_{0.24-0.59})TiO_3$	granite (in vugs)	3
Namaqualand, South Africa	$(Zn_{0.04-0.42}Fe_{0.39-0.78}Mn_{0.10-.22})TiO_3$	quartz-gahnite-spessartine rock	4
Death Valley	$(Zn_{0.17-0.81}Fe_{0.18-0.64}Mn_{0.01})TiO_3$	kyanite schist	5
	$(Zn_{0.01-0.12}Fe_{0.85-0.98}Mn_{0.01-0.02})TiO_3$		

references: 1 = Birch *et al.* (1988), 2 = Plimer (1990), 3 = Suwa *et al.* (1987), 4 = J.M. Moore, written communication (1992), 5 = present study.

GEOLOGICAL SETTING

The metapelitic rocks that are the focus of this study form a minor (<0.1%) part of the footwall of the Badwater Turtleback core complex in the Black Mountains of Death Valley (Fig. 1). Metamorphic episodes in the Precambrian, Mesozoic, and Cenozoic (late Tertiary) are inferred to have been important in the history of these rocks (Wright *et al.* 1991). In addition to the kyanite-bearing pelitic schist, other metamorphic rocks of the footwall are mylonitic quartzofeldspathic gneiss, granitic pegmatite, and marble. The age of the gneiss, marble,

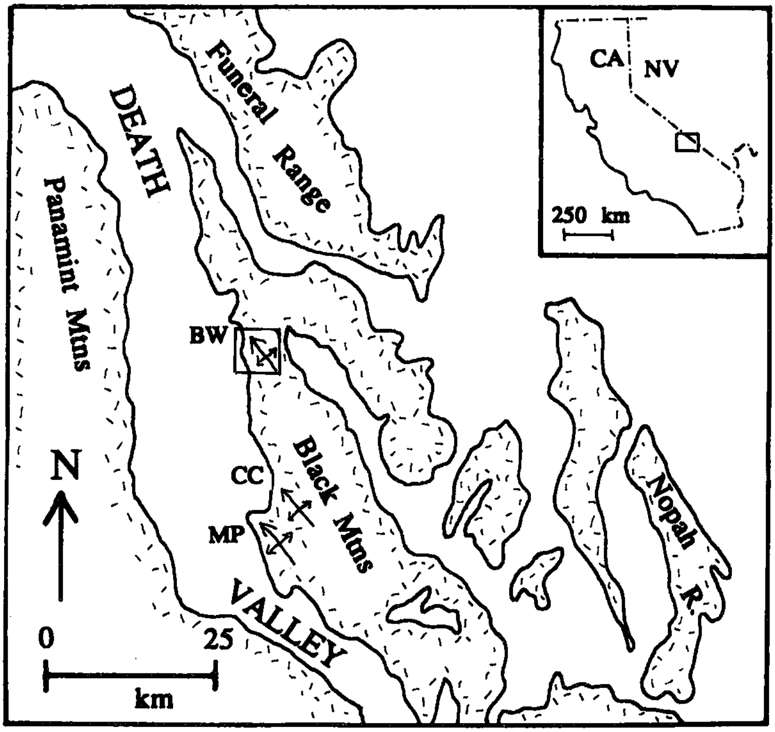

FIG. 1. Generalized map of the central Death Valley region, showing the approximate location of the outcrop bearing the zincian ilmenite – ecandrewsite solid solution (small box). BW: Badwater Turtleback, CC: Copper Canyon, MP: Mormon Point.

and pelitic rocks is Precambrian, but the pegmatites may have been emplaced during a late Tertiary episode of extension (Miller 1991).

ANALYTICAL METHODS

Electron-microprobe analyses were carried out with a JEOL 733 microprobe at the University of Washington using an accelerating voltage of 15 kV and a sample current of 20 nA. Both Bence–Albee (Bence & Albee 1968, Albee & Ray 1970) and ZAF correction methods were used, although only results obtained using the Bence–Albee method are reported in this paper. Minerals analyzed were ilmenite–ecandrewsite, garnet, biotite, muscovite, chloritoid, kyanite, and staurolite. Whole-rock X-ray-fluorescence analyses were performed at Washington State University (sample TB89–105) and at the University of Calgary (samples TB89–105b, TB91–1a).

The unit-cell dimensions of an ilmenite grain containing 10 mol% $ZnTiO_3$ were derived from centering the positions of 25 peaks with a Syntex P$\bar{1}$ single-crystal X-ray diffractometer at the University of Washington. Attempts to isolate a suitable (largely unaltered) grain of ecandrewsite for X-ray study were unsuccessful.

PETROGRAPHY AND MINERAL COMPOSITIONS

The outcrop of metapelitic schist in the Badwater Turtleback is compositionally layered on a meter scale. All layers examined contain $(Zn,Fe)TiO_3$, but only one layer was found to contain nonopaque ilmenite–ecandrewsite solid solution. Because single grains range in composition from ilmenite (<50 mol% $ZnTiO_3$) to ecandrewsite (>50 mol% $ZnTiO_3$), we refer to the nonopaque grains as ilmenite–ecandrewsite solid solution. In this layer, ilmenite–ecandrewsite coexists with a second population of opaque ilmenite (hereafter referred to as zincian ilmenite) that is less enriched in zinc than the nonopaque ilmenite–ecandrewsite. Samples TB89–105 and TB91–1a were collected from this layer. Other minerals present are kyanite, garnet, muscovite, quartz, monazite, biotite, chlorite (secondary), graphite, zircon, and titanite. Other layers in the same outcrop contain zincian ilmenite but lack ilmenite–ecandrewsite, and consist of chloritoid, twinned rutile, and relict zincian staurolite in addition to the above-listed minerals. Sample TB89–105b was collected from this layer.

Table 2 shows whole-rock compositions (major and trace elements) for the three samples listed above, as determined by X-ray fluorescence. The mineralogy and petrology of the outcrop are described below.

TABLE 2. WHOLE-ROCK COMPOSITIONS*

	TB89-105**	TB89-105b§	TB91-1a‡
SiO_2	50.99	46.05	49.43
TiO_2	1.44	1.21	1.95
Al_2O_3	27.73	32.51	30.39
Fe_2O_3	10.39	9.24	9.16
MnO	0.12	0.37	0.11
MgO	0.61	0.79	0.76
CaO	0.17	0.38	0.08
Na_2O	0.41	0.80	0.43
K_2O	4.94	5.21	5.11
P_2O_5	0.08	0.10	0.06
LOI	n.d.	2.84	3.71
total	96.89	99.50	101.19
Ni	29	37	17
Cr	121	160	192
Sc	37	n.d.	n.d.
V	198	237	330
Ba	663	1180	588
Rb	148	119	164
Sr	110	244	92
Zr	258	212	396
Y	69†	176	57
Nb	40†	21	48
Ga	37†	37†	50†
Cu	54	n.d.	n.d.
Zn	**520†**	**495†**	**975**
Pb	460†	512†	76†
La	86	65	75
Ce	198	n.d.	n.d.
Th	25	24	31

* obtained by x-ray fluorescence.
** ilmenite-ecandrewsite-bearing.
§ zincian ilmenite-bearing.
‡ ilmenite-ecandrewsite-bearing.
† values are beyond the calibration range for the standard used in analysis.
LOI = loss on ignition;
n.d. = not determined.

Ilmenite–ecandrewsite solid solution

In sample TB89–105, this type of ilmenite makes up 3–5 modal % of the rock, as determined by point-counting 1000 points on a standard thin section. Unlike other examples of zincian ilmenite or ecandrewsite reported in the literature (Birch *et al.* 1988, Plimer 1990), the ilmenite–ecandrewsite from Death Valley is not opaque; it is deep orange-brown in transmitted light, uniaxial, and optically positive. The translucence may be caused by dilution of high-absorption Fe^{2+} with zero-spin Zn^{2+}.

Grains of ilmenite–ecandrewsite are relatively large (up to 1 mm), and typically occur as polycrystalline aggregates (Figs. 2a, b). Most of the grains in the Death Valley schist are associated with garnet, either as inclusions (Fig. 2c) or intergrowths with garnet (Fig. 2d). Some matrix grains are intergrown with kyanite. Monazite, muscovite, and titanite (rare) are present as inclusions. Because abundant grains of ilmenite–ecandrewsite occur in the matrix, and because garnet containing ilmenite–ecandrewsite inclusions are extensively fractured and disaggregated (Figs. 2c, d), these inclusions are not interpreted to be an early-formed phase.

Back-scattered electron (BSE) images illustrate the extent to which ilmenite–ecandrewsite grains in the Death Valley schist have been replaced by a Fe–Ti phase

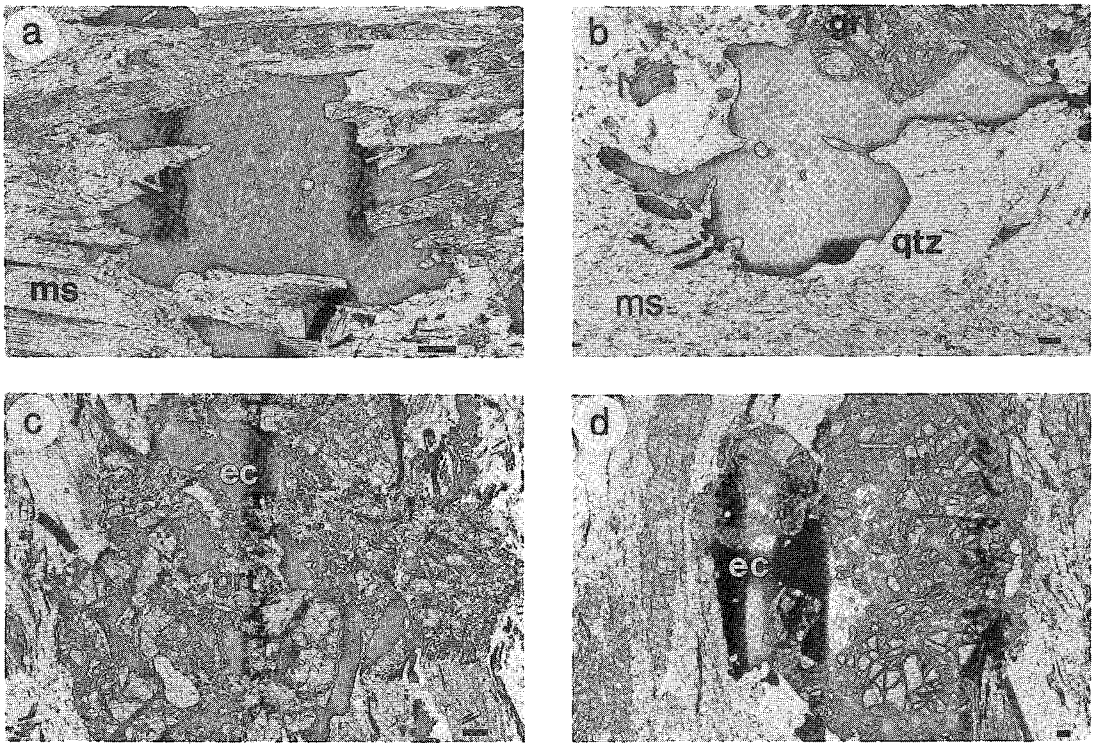

FIG. 2. Ilmenite–ecandrewsite from sample TB89–105. The grain in (a) appears lighter than the grain in (b) because it is from a thinner part of the thin section. The light-colored inclusion in (b) is monazite. Symbols: grt garnet, ky kyanite, ms muscovite, qtz quartz. (c) Ilmenite–ecandrewsite (ec) inclusions in garnet (grt). (d) Ilmenite–ecandrewsite intergrown with garnet. Scale bars: 100 μm.

or phases (Figs. 3a–d) containing minor amounts of Zn (0–4 wt% ZnO). Microprobe analyses suggest that this material may consist primarily of goethite + rutile. Attempts to identify the alteration phases by powder X-ray diffraction were unsuccessful because of an insufficient amount of sample. Most grains of ilmenite–ecandrewsite are rimmed by alteration phases, which also are present along cracks (Figs. 3a, b). Some grains have been almost completely replaced (Fig. 3d).

Because ilmenite–ecandrewsite and the alteration material are not easily distinguished in transmitted light, they were considered to be a single phase during point counting. The observation that the alteration phases lack substantial amounts of zinc is consistent with the inference that the whole-rock value for zinc (~500–975 ppm; Table 2) is lower than would be predicted for a rock containing 3–5 modal % of unaltered zincian ilmenite or ecandrewsite of the compositions observed in this rock.

The ilmenite–ecandrewsite solid solution in the Death Valley pelitic schist ranges in composition from 17 to 81 mol% $ZnTiO_3$ (Table 3). Titanium content varies from 48 to 54 wt% TiO_2, but is essentially constant at one atom p.f.u., indicating that there is very little Fe^{3+} in the ilmenite–ecandrewsite. Grains are irregularly zoned with respect to iron and zinc (Fig. 4). Single grains vary by as much as 47 mol% $ZnTiO_3$, although within any single "patch" of ilmenite (surrounded by alteration material), the maximum variation is 26 mol% $ZnTiO_3$.

Compositional profiles illustrate that the zinc content increases at contacts with alteration material (*i.e.*, at the rim and along cracks: Fig. 4). The increase in zinc near the rim and adjacent to cracks also can be observed in a BSE image (Fig. 5) of part of the grain shown in Figure 3a. The relation between zoning and the location and orientation of fractures in the ilmenite–ecandrewsite indicates that zoning is related to alteration. Although the highest contents of zinc do not represent primary compositions, the bulk zinc content of the ilmenite–ecandrewsite must have been high prior to replacement.

Figure 6 illustrates the nearly perfect one-for-one substitution of zinc for iron over the entire compositional range of the ilmenite–ecandrewsite series, indicating that there is essentially complete solid-solution between the iron and zinc end-members of the ilmenite group. Minor concentrations of manganese account for the slight deviation from the Zn = Fe line.

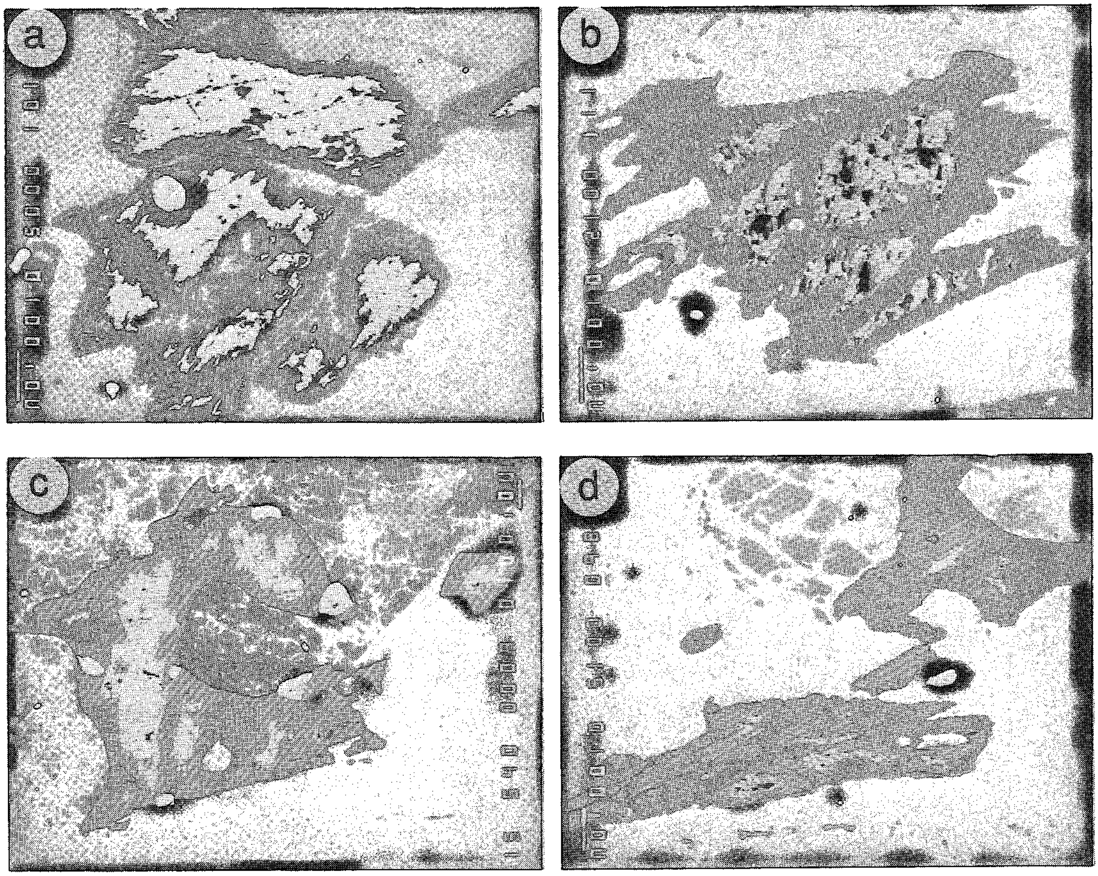

FIG. 3. (a) Back-scattered electron (BSE) image of ilmenite–ecandrewsite (white; see photomicrograph in Fig. 2b) showing partial alteration to Fe–Ti phase(s) (various shades of gray). Note the "layered" structure and variation in intensity of brightness of the alteration material, indicating compositional variation. The "patch" of ilmenite on the right in the lower grain is imaged in more detail in Figure 5. (b, c) BSE images of grains shown in Figures 2a and d, respectively. (d) Former grain of ilmenite almost completely replaced by zinc-poor alteration material. The upper grain is intergrown with garnet. Scale bars: 100 μm.

Zincian ilmenite

In the Death Valley schist, ilmenite that is petrographically and compositionally distinct from the ilmenite–ecandrewsite is present, and is referred to here as zincian ilmenite. The zincian ilmenite coexists with ilmenite–ecandrewsite and also occurs in chloritoid-bearing layers that lack ilmenite–ecandrewsite. Such ilmenite is opaque and ranges in composition from 0 to 12 mol% $ZnTiO_3$ (Table 4). Individual grains are nearly homogeneous (average $\Delta ZnTiO_3 < 2$ mol %; maximum: 7 mol %), but there is variation in composition among grains (Table 4). The unit cell of a single crystal with the composition $Fe_{0.89}Zn_{0.10}Mn_{0.01}TiO_3$ is *a* 5.064(2), *c* 14.057(6) Å.

Although there is no overlap in composition between the ilmenite–ecandrewsite solid solution and zincian ilmenite, there is nearly a continuum in composition between the two populations, from <1 to 81 mol% $ZnTiO_3$ (Fig. 6). Compositions of zincian ilmenite and ecandrewsite from Australia and Spain (Birch *et al.* 1988, Plimer 1990) also span a significant compositional range (Table 1). This range suggests that, as noted above, complete isomorphic solid-solution between the iron and zinc end-members of the ilmenite group is possible.

Garnet

The garnet is almandine-rich (~87 mol%); the grains are essentially unzoned (Table 5). It contains trace amounts of zinc (less than 0.13 wt% ZnO; Table 5), and there is no detectable change in zinc content in the garnet adjacent to ilmenite–ecandrewsite. Grains of garnet are extensively fractured, embayed, and have been partially

TABLE 3. REPRESENTATIVE COMPOSITIONS OF ILMENITE-ECANDREWSITE*

	Ia	Ib	Ic	Id	Ie	If	Ig	Ih	Ij
TiO_2	50.01	53.11	51.05	48.47	53.08	52.07	53.89	53.02	50.24
Al_2O_3	0.04	0.03	0.00	0.04	0.00	0.03	0.01	0.01	0.01
FeO	15.34	28.85	17.64	8.31	24.89	21.00	36.50	33.47	12.37
MnO	0.61	0.62	0.55	0.62	0.59	0.63	0.72	0.69	0.65
MgO	0.09	0.08	0.09	0.08	0.09	0.09	0.06	0.06	0.09
ZnO	34.08	17.19	30.60	43.17	21.49	26.07	8.95	13.27	36.67
total	100.2	99.88	99.93	100.7	100.1	99.89	100.1	100.5	100.0
cations									
Ti	0.99	1.02	1.00	0.97	1.02	1.01	1.02	1.01	1.00
Al	0.00	0.00	0.00	0.00	0.00	0.00	0.00	0.00	0.00
Fe	0.34	0.62	0.39	0.19	0.53	0.46	0.77	0.71	0.27
Mn	0.01	0.01	0.01	0.01	0.01	0.01	0.02	0.02	0.02
Mg	0.00	0.00	0.00	0.00	0.00	0.00	0.00	0.00	0.00
Zn	0.66	0.32	0.59	0.85	0.41	0.50	0.17	0.25	0.71
mol%									
Ilm§	33.20	64.38	38.87	17.61	55.77	46.85	80.69	72.78	27.13
Prn	1.34	1.41	1.24	1.34	1.35	1.43	1.62	1.53	1.45
Ecd	65.10	33.87	59.52	80.73	42.51	51.35	17.47	25.48	71.05

* All analyses are from a single grain in sample TB89-105 that spans the entire compositional range exhibited by all analyzed grains. Trace amounts of Si, Nb are present; Cr not detected.

§ Ilm = ilmenite (Fe) component; Prn = pyrophanite (Mn) component; Ecd = ecandrewsite (Zn) component.

replaced by chlorite and sericite. Extensive staining by hematite occurs along fractures. In TB89–105, ilmenite–ecandrewsite is the most abundant inclusion in garnet (Fig. 2c), although rare inclusions of quartz also are present. In the chloritoid-bearing layer (TB89–105b), garnet contains inclusions of staurolite (Table 6).

Biotite

Pale brown biotite is confined to thin discontinuous layers in the ilmenite–ecandrewsite-bearing sample (<2 modal % of the rock); it contains only trace amounts of zinc (<0.10 wt% ZnO; Table 6). Some grains of biotite have been altered to chlorite, which makes up 3–4 modal % of the rock. In addition to a lack of textural evidence for equilibrium between garnet and biotite, anomalous, unreasonable results of garnet–biotite geothermometry suggest that garnet and biotite are not in equilibrium (see below).

Muscovite

Muscovite makes up almost 40% of sample TB89–105, and is the most abundant mineral in the rock. It occurs both as coarse grains and as fine-grained aggregates that may represent a pseudomorph after plagioclase (there is no plagioclase in the rock at present). Microprobe analyses indicate that the muscovite contains substantial amounts of Ti (nearly 2 wt% TiO_2), as well as Fe and Mg, but no zinc (Table 6).

Kyanite

Kyanite is abundant in sample TB89–105 (11 modal %). Microprobe analyses indicate the presence of 0.12–0.38 wt% Fe_2O_3. Kyanite is generally unaltered, but some grains are rimmed by sericite, and contain inclu-

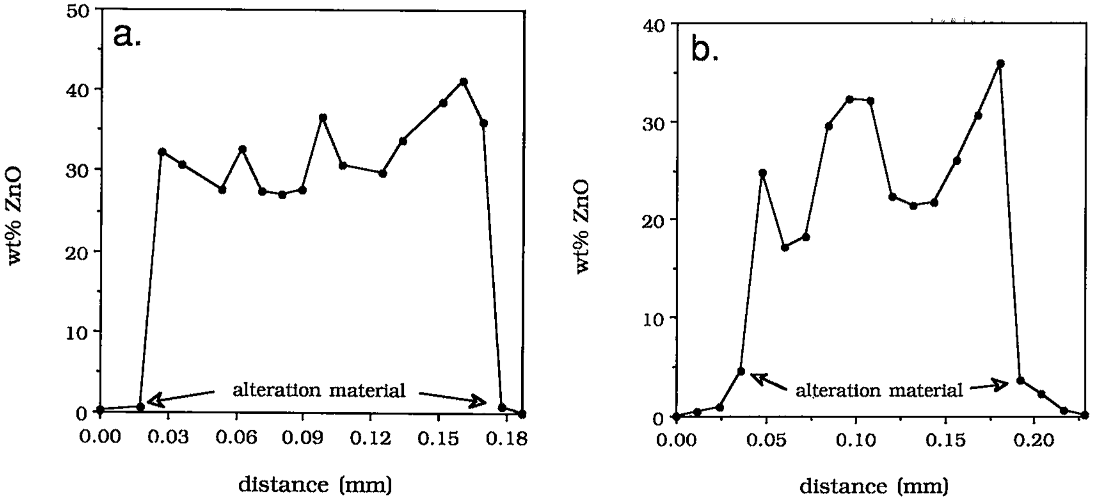

FIG. 4. (a, b) Composition profiles of ilmenite–ecandrewsite. Note that the Zn content of ilmenite–ecandrewsite increases near contact with low-Zn alteration material. Zn "spikes" in interior of the grains correspond to compositions obtained near cracks filled with alteration material. The Zn content of the alteration material in (b) may be artificially high near ilmenite–ecandrewsite because of interference effects.

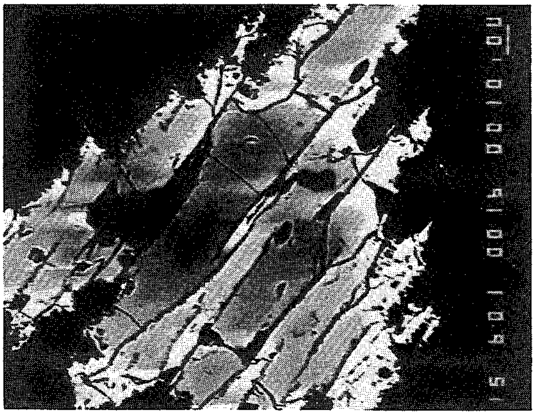

FIG. 5. Back-scattered electron image illustrating Fe–Mn zoning in part of the ilmenite–ecandrewsite grain shown in Figures 2b and 3a. Lighter areas are the most zinc-rich. The black area surrounding the image is Zn-poor alteration material. Scale bar: 100 µm.

sions of muscovite. Some grains are intergrown with ilmenite–ecandrewsite.

Staurolite

Fe-rich staurolite containing 3 wt% ZnO (Table 6) is present as relict grains in the chloritoid + zincian ilmenite-bearing layer (TB89–105b); no staurolite was observed in the ilmenite–ecandrewsite-bearing layer (TB89–105). The staurolite in TB89–105b is interpreted to be relict because it occurs as inclusions in chloritoid and garnet, and as small, irregularly shaped grains in the matrix.

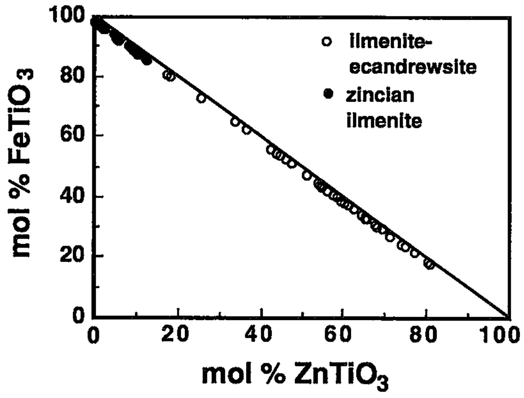

FIG. 6. Graph of mol% $FeTiO_3$ *versus* $ZnTiO_3$ in both types of ilmenite from the Death Valley schist. Solid line: perfect one-to-one substitution of Fe and Zn. Slight deviation of data from the solid line is the result of the presence of small amounts of Mn.

TABLE 4. REPRESENTATIVE COMPOSITIONS OF ZINCIAN ILMENITE*

	1	2	3	4	5	6	7
TiO_2	53.23	52.56	52.36	52.43	52.57	52.49	52.77
Al_2O_3	0.01	0.11	0.02	0.00	0.00	0.00	0.00
FeO	43.04	45.78	40.07	41.73	46.23	46.71	46.07
MnO	0.92	0.61	0.59	0.61	0.68	0.61	0.57
MgO	0.07	0.08	0.19	0.19	0.15	0.17	0.14
ZnO	2.81	1.00	6.47	5.43	0.26	0.10	0.58
total	100.08	100.14	99.70	100.39	99.89	100.08	100.13
cations							
Ti	1.01	1.00	1.00	1.00	1.00	1.00	1.00
Al	0.00	0.00	0.00	0.00	0.00	0.00	0.00
Fe	0.91	0.97	0.85	0.88	0.98	0.98	0.97
Mn	0.02	0.01	0.01	0.01	0.02	0.01	0.01
Mg	0.00	0.00	0.01	0.01	0.01	0.01	0.01
Zn	0.05	0.02	0.12	0.10	0.01	0.00	0.01
mol%							
Ilm§	92.41	96.51	85.77	87.89	97.52	97.89	97.18
Prn	2.01	1.31	1.29	1.31	1.46	1.30	1.23
Ecd	5.30	1.90	12.27	10.06	0.50	0.20	1.10

* Each analysis from a different grain in TB89-105.
§ Ilm = ilmenite (Fe) component; Prn = pyrophanite (Mn) component; Ecd = ecandrewsite (Zn) component.

P–T CONDITIONS

The ilmenite–ecandrewsite-bearing layer in the Death Valley schist lacks suitable equilibrium assemblages for geobarometric determination, but the chloritoid-bearing

TABLE 5. REPRESENTATIVE COMPOSITIONS OF GARNET FROM SAMPLE TB89-105

	1-C§	1-R	2-C	2-R	3-C	3-R
SiO_2	36.20	36.09	36.24	36.01	36.65	36.63
TiO_2	0.05	0.05	0.05	0.36	0.05	0.07
Al_2O_3	21.11	21.19	20.91	21.20	21.31	21.21
FeO	38.82	38.94	38.80	38.71	38.40	38.50
MnO	1.04	1.04	1.02	1.11	1.05	1.06
MgO	2.49	2.44	2.56	2.29	2.56	2.39
CaO	0.26	0.26	0.29	0.27	0.28	0.25
ZnO	0.13	0.11	0.09	0.11	0.08	0.09
total	100.10	100.12	99.96	100.06	100.38	100.20
cations						
Si	2.95	2.94	2.96	2.94	2.97	2.97
Ti	0.00	0.00	0.00	0.02	0.00	0.00
Al	2.03	2.04	2.01	2.04	2.03	2.03
Fe	2.65	2.66	2.65	2.64	2.60	2.61
Mn	0.07	0.07	0.07	0.08	0.07	0.07
Mg	0.30	0.30	0.31	0.28	0.31	0.29
Ca	0.02	0.02	0.03	0.02	0.03	0.02
Zn	0.10	0.01	0.01	0.01	0.01	0.01
mol%						
Alm*	86.71	86.94	86.48	87.23	86.34	87.02
Sps	2.36	2.36	2.31	2.54	2.40	2.44
Pyr	9.93	9.72	10.18	9.21	10.27	9.64
Grs	0.76	0.76	0.84	0.79	0.82	0.71

§ C = core; R = rim.
* symbols of Kretz (1983).

TABLE 6. REPRESENTATIVE COMPOSITIONS OF ADDITIONAL MINERALS

	biotite	muscovite	staurolite (in cld)	staurolite (matrix)	garnet (core)	garnet (rim)	chloritoid
SiO_2	32.42	46.92	28.24	28.50	37.27	36.84	24.85
TiO_2	1.38	1.81	0.59	0.58	0.16	0.05	0.00
Al_2O_3	16.45	33.33	53.75	53.11	20.95	20.77	40.96
FeO	29.39	1.48	11.77	11.02	35.76	35.97	24.70
MnO	0.09	0.00	0.08	0.09	1.94	2.73	0.20
MgO	5.44	0.76	1.23	1.34	3.03	2.12	2.57
ZnO	0.08	0.00	2.72	3.40	0.00	0.00	0.00
CaO	0.09	0.00	0.00	0.00	1.14	1.17	n.a.
Na_2O	0.00	0.26	0.00	0.00	n.a.	n.a.	n.a.
K_2O	8.45	10.35	0.00	0.00	n.a.	n.a.	n.a.
Cl	1.40	0.00	n.a.	n.a.	n.a.	n.a.	n.a.
F	0.09	0.00	n.a.	n.a.	n.a.	n.a.	n.a.
total	95.28	94.91	98.38	98.04	100.25	99.65	93.28
basis:	22 atoms of oxygen		47 atoms of oxygen		12 atoms of oxygen		
Si	5.31	6.27	7.99	8.01	3.00	3.00	2.03
Ti	0.17	0.18	0.12	0.12	0.00	0.00	0.00
Al	3.18	5.24	17.92	17.80	1.99	2.00	3.95
Fe	4.03	0.17	2.78	2.62	2.41	2.45	1.69
Mn	0.01	0.00	0.02	0.02	0.13	0.19	0.01
Mg	1.33	0.15	0.52	0.57	0.36	0.26	0.31
Zn	0.01	0.00	0.57	0.71	0.00	0.00	0.00
Ca	0.02	0.00	0.00	0.00	0.10	0.10	------
Na	0.00	0.07	0.00	0.00	------	------	------
K	1.77	1.76	0.00	0.00	------	------	------
Cl	0.38	0.00	------	------	------	------	------
F	0.05	0.00	------	------	------	------	------
X*							
Fe	0.667		0.715	0.668	0.802	0.817	0.838
Mg	0.220		0.134	0.145	0.121	0.856	0.155
Zn	0.002		0.147	0.181	0.000	0.000	0.000

*** Mole fractions calculated as follows: biotite: M/(Fe + Mn + Mg + Ti + ^{VI}Al + Zn); staurolite, chloritoid: M/(Fe + Mn + Mg + Zn); garnet: M/(Fe + Mn + Mg + Ca), where M represents Fe, Mg, Zn.**

layer contains the assemblage garnet – rutile – aluminosilicate – ilmenite – quartz (GRAIL), which may be used to estimate pressure of metamorphism (Bohlen *et al.* 1983). The activity of almandine in garnet was calculated using the model of Berman (1990), and the activity of $FeTiO_3$ in ilmenite was calculated assuming ideal mixing between $FeTiO_3$ and $ZnTiO_3$. At 500–600°C (see below), the calculated pressure is 7 ± 1 kbar. Because the ilmenite–ecandrewsite-bearing layer is present in the same outcrop, this pressure is inferred for it as well. The calculated pressure is in accord with values of 6.5 ± 1 kbar obtained for Mesozoic metamorphism of kyanite-bearing rocks in the northern Funeral Range (Fig. 1) (Labotka & Albee 1988).

Because garnet and biotite are not in equilibrium in the Death Valley schist, it was not possible to calculate a reasonable temperature of metamorphism using garnet–biotite geothermometry. Garnet–ilmenite thermometry (Pownceby *et al.* 1987), which is based on Fe–Mn exchange between garnet and ilmenite, gave similarly unreasonable (>2000°C) results, perhaps because of the small amount of Mn present in garnet and ilmenite. However, an estimate of *minimum* temperature of 500°C (assuming ideal mixing in staurolite and chloritoid) is indicated by the reaction

$$2\ \text{staurolite} + \text{quartz} + 2H_2O = 4\ \text{chloritoid} + 5\ Al_2SiO_5 \qquad (1)$$

which has a steep slope in P–T space. The position of this reaction was calculated using mineral compositions from the Death Valley pelitic schist and the program GEØ–CALC (Berman *et al.* 1987).

The maximum temperature is constrained by the absence of sillimanite. Assuming that pressure did not exceed 7.5 kbar, the temperature could not have exceeded 675°C, which is somewhat lower than temperatures estimated for the ecandrewsite-bearing rocks from Broken Hill (Plimer 1990).

DISCUSSION

Ilmenite–ecandrewsite solid solution is the only mineral that hosts substantial amounts of zinc in the staurolite-free layer of the Death Valley schist. The discussion that follows is concerned with the stability of minerals with the ilmenite structure containing greater than trace amounts of the $ZnTiO_3$ component. Therefore, although we specifically refer only to the stability of *zincian ilmenite* (<50 mol % $ZnTiO_3$), the interpretations implicitly apply to ecandrewsite (>50 mol % $ZnTiO_3$) as well.

Paragenesis of zincian ilmenite

Three of the known occurrences of zincian ilmenite – ecandrewsite solid solution are from regionally metamorphosed metalliferous metasedimentary rocks (Broken Hill, Namaqualand, Death Valley; Table 1). Plimer (1990) argued, from field and textural evidence, that zincian ilmenite – ecandrewsite formed by reaction of rutile, anatase, or ilmenite with zincian clays or carbon-

TABLE 7. ESTIMATED THERMODYNAMIC PROPERTIES

	$ZnTiO_3$	$ZnAl_2O_4$
$\Delta\overline{H}^o_{f\,298}$ (kJ)	-1301.9*	-2071.1†
S° (J/K)	94.93*	87.89†
$\overline{V}$ (J/bar)	3.119§	3.978‡
Heat Capacity**		
k_0	95.797	200.357
k_1	7.286×10^{-3}	7.286×10^{-3}
k_2	0	-8.284×10^{2}
k_3	-33.678×10^{5}	-38.614×10^{5}
k_4	40.3511×10^{7}	40.851×10^{7}

Reference state is 298.15 K, 1 bar. ($\Delta\overline{H}^o_{f\,298}$) from elements.

*Derived from combination of free energy of formation from oxides (Jacob & Alcock 1975) with properties of ZnO (Pankratz 1982) and TiO_2 (Berman 1988).

† Derived from combination of free energy of formation from oxides (Jacob 1976) with properties of ZnO (Pankratz 1982) and Al_2O_3 (Berman 1988).

§ Bartram & Sleptys (1961).

‡ Waychunas (1991).

** $Cp = k_0 + k_1 * T + k_2 * T^{-1/2} + k_3 * T^{-2} + k_4 * T^{-3}$ (estimated from sum of oxides).

ates during prograde metamorphism. Alternatively, (Zn,Fe)TiO_3 may form from desulfidation of sphalerite or by breakdown of zinc-bearing minerals such as staurolite, biotite, or högbomite, in a manner similar to what has been proposed for the formation of zincian spinel (*e.g.*, Stoddard 1979, Dietvorst 1980, Spry & Scott 1986). Zincian ilmenite also occurs in vugs in granite in Fuzhou, China (Suwa *et al.* 1987; Table 1), which indicates that zincian ilmenite also may precipitate directly from hydrothermal solution.

Zincian ilmenite – ecandrewsite solid solution is apparently rare, in contrast to gahnite ($ZnAl_2O_4$), which is a relatively common mineral in regionally metamorphosed pelitic rocks (*e.g.*, Robinson & Jaffe 1969, Loomis 1972, Frost 1973, Atkin 1978, Stoddard 1979, Dietvorst 1980). Gahnite commonly coexists with ilmenite (*e.g.*, Frost 1973, Stoddard 1979), but gahnite coexisting with zincian ilmenite – ecandrewsite has been reported only from Broken Hill, Australia (Birch *et al.* 1988, Plimer 1990) and Namaqualand, South Africa (J.M. Moore, written comm., 1992). In order to understand the occurrence of zincian ilmenite, it is therefore desirable to determine what conditions, if any, might favor partitioning of zinc into ilmenite, relative to spinel (gahnite).

Although not observed in the Death Valley schist or any other locality of zincian ilmenite described in the literature, zincian högbomite is present in some metapelitic rocks (Petersen *et al.* 1989), and is a possible precursor mineral to zincian ilmenite (J.M. Moore, written comm., 1992). The relative stability of zinc-bearing högbomite and ilmenite is therefore also of interest. However, in the absence of well-characterized occurrences of coexisting zincian högbomite and zincian ilmenite, we confine our discussion to the stability of zincian ilmenite relative to gahnite.

The Zn–Fe exchange equilibrium between ilmenite and aluminate spinel,

$$\underset{\text{ilmenite}}{ZnTiO_3} + \underset{\text{spinel}}{FeAl_2O_4} = \underset{\text{ilmenite}}{FeTiO_3} + \underset{\text{spinel}}{ZnAl_2O_4} \qquad (2)$$

can be calculated using thermodynamic data for pure $ZnTiO_3$ and pure $ZnAl_2O_4$ listed in Table 7 and by approximating Fe–Zn mixing in ilmenite and spinel solutions as ideal. This approximation may be warranted because of the small difference in ionic radius between Zn^{2+} and Fe^{2+} (0.025 Å: Shannon & Prewitt 1969) and because $FeAl_2O_4$ and $ZnAl_2O_4$ both have the structure of normal spinel (Waychunas 1991). The properties of $FeTiO_3$ are taken from Berman (1988), and those of $FeAl_2O_4$, from Sack & Ghiorso (1991). Calculated distribution-isotherms (Fig. 7) predict that zincian ilmenite will coexist with aluminate spinel only if the spinel is nearly pure $ZnAl_2O_4$ or if temperatures are significantly higher than are typically attained during regional metamorphism (>800°C). The calculations were performed assuming that extent of incorporation of ferric iron in spinel and ilmenite is insignificant, which should be reasonable for the fugacity of oxygen encountered in a graphite-bearing pelitic schist. Even if the oxides contained significant levels (10 mol %) of the hematite and franklinite ($ZnFeO_4$) components, the position of the distribution-isotherms is not likely to be strongly affected.

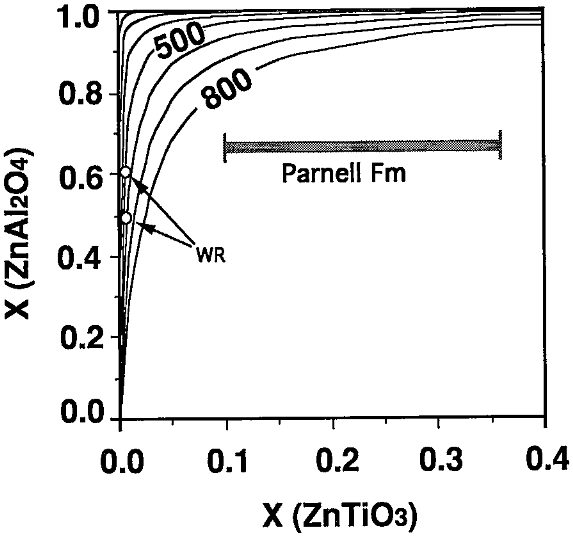

FIG. 7. Calculated isotherms for Zn–Fe exchange between ilmenite and gahnite, compared with observed compositions from the Parnell Formation, Broken Hill (Plimer 1990) and from the Wind River Range (WR), Wyoming. Gahnite compositions for WR from Frost (1973); ilmenite compositions determined in the present study from samples provided by B.R. Frost.

The calculated distribution-isotherms are inconsistent with observed compositions of coexisting gahnite and ilmenite from the Parnell Formation of the Broken Hill area (Plimer 1990), in which gahnite of intermediate composition coexists with zincian ilmenite and ecandrewsite (Fig. 7). This finding suggests that the gahnite and zincian ilmenite (and ecandrewsite) in the Parnell Formation are not in equilibrium, or that the thermodynamic predictions are incorrect. In order to test the validity of the thermodynamic calculations, we determined the composition of ilmenite coexisting with ferroan gahnite from quartz–biotite schists in the Wind River Range, Wyoming (Frost 1973). The Zn content of the ilmenite is below the detection limit for analysis by electron microprobe (0.08% ZnO), which is less than predicted for the temperatures of peak metamorphism in these schists (625 ± 50°C, calculated from garnet and biotite compositions reported by Frost 1973) (Fig. 7). This discrepancy could result from retrograde re-equilibration of these phases or from inaccuracies in the thermodynamic data, but the calculated distribution of zinc between ilmenite and aluminate spinel is approximately consistent with the compositions of coexisting oxides from Wyoming. It is therefore probable that the coexisting oxides from the Parnell Formation (Plimer 1990) are not in equilibrium.

Because gahnite has not been observed in the Death Valley schist, we investigated the effect of zinc on the stability of ilmenite relative to gahnite in metapelitic rocks according to the reaction

$$\underset{\text{ilmenite}_{ss}}{ZnTiO_3} + \underset{\text{kyanite}}{Al_2SiO_5} = \underset{\text{spinel}_{ss}}{ZnAl_2O_4} + \underset{\text{quartz}}{SiO_2} + \underset{\text{rutile}}{TiO_2} \qquad (3)$$

using thermodynamic data listed in Table 7 and the properties of kyanite, quartz and rutile from Berman (1988). The calculations indicate that even at a high temperature (800°C), only small amounts of the $ZnTiO_3$ component (<3.5 mol%) may be dissolved in ilmenite before the ilmenite is destabilized relative to gahnite, quartz and rutile, and that the solubility limit is considerably less at a lower temperature (Fig. 8). In other words, if the assumed thermodynamic properties of the minerals are accurate, then zincian ilmenite from the Death Valley locality must have been metastable with respect to gahnite, quartz, and rutile over the entire range of estimated conditions of metamorphism. This result is insensitive to pressure, varying only a few tenths of a mol % between 0.001 and 10 kbar. Under oxidizing conditions, ilmenite could be slightly stabilized by incorporation of minor amounts of Fe_2O_3, but concomitant incorporation of Fe^{3+} into spinel would probably leave the position of the phase boundary largely unaffected. As noted above, the electron-microprobe data indicate that the Fe_2O_3 component in ilmenite from Death Valley is negligible.

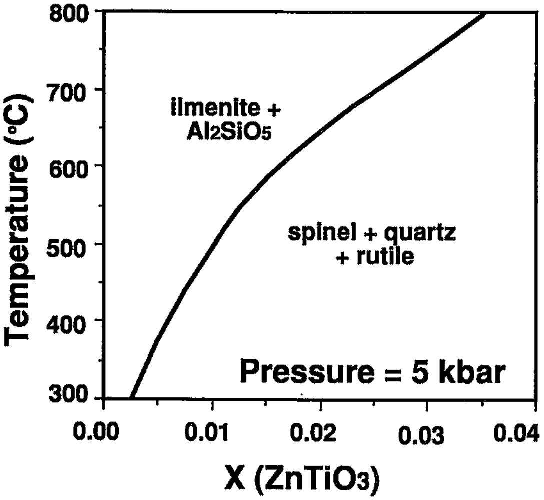

FIG. 8. Limit of solubility of $ZnTiO_3$ in ilmenite coexisting with aluminosilicate before assemblage aluminate spinel + quartz + rutile is stabilized, under the assumption that ilmenite and spinel must be in Fe–Zn exchange equilibrium according to reaction (2). The very small change in volume associated with this reaction indicates that the location of the reaction boundary is insensitive to pressure.

The results of the thermodynamic calculations are in accord with the crystal chemistry of Zn^{2+} in silicates and oxides; Zn^{2+} is generally more stable in tetrahedral coordination than in octahedral coordination (Neumann 1949). It is therefore not surprising that Zn^{2+} concentrates in the tetrahedral sites of minerals such as spinel, staurolite, and högbomite rather than in the octahedrally coordinated sites of the ilmenite structure.

Disagreement between the observed compositions of zincian ilmenite and thermodynamic calculations, and between compositions of ilmenite coexisting with gahnite in the Wind River schists, suggests that zinc-rich ilmenite may be metastable relative to gahnite in aluminous metasedimentary rocks. Metastable phases are not generally believed to persist during an extended period of regional metamorphism. We therefore contend that ilmenite containing more than a few mol % $ZnTiO_3$ in this area and in other regionally metamorphosed metasedimentary rocks formed during short-lived metasomatic events that postdated the peak of regional metamorphism. At the Death Valley locality, this interpretation is supported by the presence of late-stage dikes of granitic pegmatite that cross-cut the pelitic schist and may have provided fluids for the metasomatic event.

The enrichment of $ZnTiO_3$ associated with formation of Zn-poor alteration material around rims and along cracks in ilmenite–ecandrewsite from Death Valley demonstrates that some portion of the zinc enrichment is caused by late retrograde alteration. Plimer (1990) also observed enrichment of $ZnTiO_3$ at grain boundaries and attributed this effect to retrograde metamorphism. On the other hand, it should be noted that the essentially unaltered zincian ilmenite also is richer in $ZnTiO_3$ than the calculated limit of stability. Both types of ilmenite from Death Valley may therefore have formed during metasomatic events, even though petrographic evidence for alteration or metasomatism is lacking for zincian ilmenite. Based on this inference and the above calculations, we conclude that ilmenite with a significant proportion of the $ZnTiO_3$ component is metastable in metamorphic environments.

ACKNOWLEDGEMENTS

We thank S.E. Haggerty, Bernard W. Evans, John Moore, and an anonymous reviewer for helpful comments. B. Ronald Frost kindly provided the Wind River sample. We also thank John M. Moore for permission to include his occurrence of zincian ilmenite in Namaqualand in our paper. MGM thanks Mark Savoca for assistance in the field. Terry Swanson provided valuable analytical assistance in the early stages of this investigation. X-ray-fluorescence analyses were performed by Diane Johnson at Washington State University and Pat Michael at the University of Calgary. Support for completion of the manuscript was provided by an NSERC Operating Grant to E.D. Ghent at the University of Calgary while the first author was a postdoctoral fellow at the University of Calgary.

REFERENCES

ALBEE, A.L. & RAY, L. (1970): Correction factors for electron probe microanalysis of silicates, oxides, carbonates, phosphates, and sulfates. *Anal. Chem.* **42**, 1408-1414.

ATKIN, B.P. (1978): Hercynite as a breakdown product of staurolite from within the aureole of the Ardara Pluton, County Donegal, Eire. *Mineral. Mag.* **42**, 237-239.

BARTRAM, S.F. & SLEPTYS, R.A. (1961): Compound formation and crystal structure in the system $ZnO–TiO_2$. *J. Am. Ceram. Soc.* **44**, 493-499.

BENCE, A.E. & ALBEE, A.L. (1968): Empirical correction factors for electron microanalysis of silicates and oxides. *J. Geol.* **76**, 382-403.

BERMAN, R.G. (1988): Internally-consistent thermodynamic data for minerals in the system $Na_2O–K_2O–CaO–MgO–FeO–Fe_2O_3–Al_2O_3–SiO_2–TiO_2–H_2O–CO_2$. *J. Petrol.* **29**, 445-522.

______ (1990): Mixing properties of Ca–Mg–Fe–Mn garnets. *Am. Mineral.* **75**, 328-344.

______, BROWN, T. & PERKINS, E. (1987): GEϕ–CALC: software for calculation and display of P–T–*X* diagrams. *Am. Mineral.* **72**, 861-862.

BIRCH, W.D., BURKE, E.A.J., WALL, V.J. & ETHERIDGE, M.A. (1988): Ecandrewsite, the zinc analogue of ilmenite, from Little Broken Hill, New South Wales, Australia, and the San Valentin Mine, Sierra de Cartagena, Spain. *Mineral. Mag.* **52**, 237-240.

BOHLEN, S.R., WALL, V.J. & BOETTCHER, A. (1983): Experimental investigations and geological applications of equilibria in the system $FeO–TiO_2–Al_2O_3–SiO_2–H_2O$. *Am. Mineral.* **68**, 1049-1058.

DIETVORST, E.J.L. (1980): Biotite breakdown and the formation of gahnite in metapelitic rocks from Kemi, southwest Finland. *Contrib. Mineral. Petrol.* **75**, 327-337.

FROST, B.R. (1973): Ferroan gahnite from quartz – biotite – almandine schist, Wind River Mountains, Wyoming. *Am. Mineral.* **58**, 831-834.

JACOB, K.T. (1976): Gibbs free energies of formation of $ZnAl_2O_4$ and $ZnCr_2O_4$. *Thermochim. Acta* **15**, 79-87.

______ & ALCOCK, C.B. (1975): Evidence of residual entropy in the cubic spinel Zn_2TiO_4. *High Temperatures – High Pressures* **7**, 433-439.

KRETZ, R. (1983): Symbols for rock-forming minerals. *Am. Mineral.* **68**, 277-279.

LABOTKA, T.C. & ALBEE, A.L. (1988): Metamorphism and tectonics of the Death Valley region, California and Nevada. *In* Metamorphism and Crustal Evolution of the Western United States (W.G. Ernst, ed.). Prentice-Hall, Englewood Cliffs, New Jersey (715-736).

LOOMIS, T.P. (1972): Contact metamorphism of pelitic rock by the Ronda ultramafic intrusion, southern Spain. *Geol. Soc. Am. Bull.* **83**, 2449-2474.

MILLER, M.G. (1991): Field evidence for syntectonic intrusive origin of mylonitic rocks in the footwall of a metamorphic core complex, Badwater Turtleback, Death Valley, California. *Geol. Soc. Am., Abstr. Programs* **23**(5), A189.

NEUMANN, H. (1949): Notes on the mineralogy and geochemistry of zinc. *Mineral. Mag.* **28**, 575-581.

PANKRATZ, L.B. (1982): Thermodynamic properties of elements and oxides. *U.S. Bur. Mines Bull.* **672**.

PETERSEN, E.U., ESSENE, E.J., PEACOR, D.R. & MARCOTTY, L.A. (1989): The occurrence of högbomite in high-grade metamorphic rocks. *Contrib. Mineral. Petrol.* **101**, 350-360.

PLIMER, I.R. (1990): The ilmenite–ecandrewsite solid solution series, Broken Hill, Australia. *Neues Jahrb. Mineral. Monatsh.*, 529-536.

POWNCEBY, M.I., WALL, V.J. & O'NEILL, H.St.C. (1987): Fe–Mn partitioning between garnet an ilmenite: experimental calibration and applications. *Contrib. Mineral. Petrol.* **97**, 116-126.

ROBINSON, P. & JAFFE, H.W. (1969): Chemographic exploration of amphibole assemblages from central Massachusetts and southwestern New Hampshire. *Mineral. Soc. Am., Spec. Pap.* **2**, 251-274.

SACK, R.O. & GHIORSO, M.S. (1991): An internally consistent model for the thermodynamic properties of Fe–Mg-titanomagnetite-aluminate spinels. *Contrib. Mineral. Petrol.* **106**, 474-505.

SHANNON, R.D. & PREWITT, C.T. (1969): Effective ionic radii in oxides and fluorides. *Acta Crystallogr.* **B25**, 925-946.

SPRY, P.G. & SCOTT, S.D. (1986): The stability of zincian spinels in sulfide systems and their potential as exploration guides for metamorphosed massive sulfide deposits. *Econ. Geol.* **81**, 1446-1463.

STODDARD, E.F. (1979): Zinc-rich hercynite in high-grade metamorphic rocks: a product of the dehydration of staurolite. *Am. Mineral.* **64**, 736-741.

SUWA, K., ENAMI, M., HIRAIWA, I. & YANG, T. (1987): Zn–Mn ilmenite in the Kuiqi Granite from Fuzhou, Fujian Province, East China. *Mineral. Petrol.* **36**, 111-120.

WAYCHUNAS, G.A. (1991): Crystal chemistry of oxides and oxyhydroxides. *In* Oxide Minerals: Petrologic and Magnetic Significance (D.H. Lindsley, ed.). *Rev. Mineral.* **25**, 11-68.

WRIGHT, L.A., THOMPSON, R.A., TROXEL, B.W., PAVLIS, T.L., DEWITT, E.H., OTTON, J.K., ELLIS, M.A., MILLER, M.G. & SERPA, L.F. (1991): Cenozoic magmatic and tectonic evolution of the east–central Death Valley region, California. *Geol. Soc. Am., Field Trip Guide.*

Received March 3, 1992, revised manuscript accepted August 4, 1992.